Journal of Analytical and Applied Pyrolysis 115 (2015) 103–111

Contents lists available at ScienceDirect

Journal of Analytical and Applied Pyrolysis

journal homepage: www.elsevier.com/locate/jaap

Pyrolysis mechanism of β—O—4 type lignin model dimer

Lei Chen [a], Xiaoning Ye [b], Feixian Luo [c], Jingai Shao [a,*], Qiang Lu [b,**], Yang Fang [a], Xianhua Wang [a], Hanping Chen [a]

[a] State Key Laboratory of Coal Combustion, Huazhong University of Science & Technology, Wuhan 430074, Hubei, PR China
[b] National Engineering Laboratory for Biomass Power Generation Equipment, North China Electric Power University, Beijing 102206, PR China
[c] Beijing National Laboratory of Molecular Sciences (BNLMS) and Key Laboratory of Bioorganic Chemistry and Molecular Engineering of Ministry of Education, College of Chemistry and Green Chemistry Center, Peking University, Beijing 100871, PR China

ARTICLE INFO

Article history:
Received 3 February 2015
Received in revised form 23 June 2015
Accepted 11 July 2015
Available online 19 July 2015

Keywords:
Lignin dimer
Py-GC/MS
Density functional theory
Pyrolysis mechanism

ABSTRACT

A β—O—4 type lignin dimer compound was synthesized, namely 1-(4-methoxyphenyl)-2-(2-methoxyphenoxy) ethanol. To elucidate its pyrolysis mechanism, analytical pyrolysis-gas chromatography/mass spectrometry (Py-GC/MS) experiments were performed to reveal the distribution of the pyrolytic products under different temperatures. Concurrently, density functional theory (DFT) calculations were conducted to analyze and verify the thermal decomposition mechanisms of the lignin dimer and the product formation pathways. The results show that the lignin dimer will undergo the Cβ—O bond homolysis to produce 4-methoxystyrene and guaiacol at low pyrolysis temperatures. Whereas at medium pyrolysis temperatures, besides the Cβ—O homolysis, Cβ—O concerted decomposition will also take place to form carbonyl-containing phenolics. At high pyrolysis temperatures, the primary pyrolytic products will undergo secondary decomposition reactions to form a complex variety of products. With the combination of the experimental results and theoretical calculations, the pyrolysis mechanism of the lignin dimer model compound is clearly interpreted in this study.

1. Introduction

Due to the depletion of fossil fuels and severe environmental issues, the utilization of biomass resources has gained widespread attention [1]. Pyrolysis is an important thermochemical method for using biomass, wherein the fast pyrolysis technique is implemented to convert biomass into crude bio-oil products [2]. Bio-oil can be directly utilized or refined as a liquid fuel, and it is also a potential feedstock for valuable chemical products [3–6]. Studies of the biomass pyrolysis mechanism can understand the pyrolysis characteristics and pathways for specific products formation, thus providing a theoretical basis for research on selective pyrolysis for high-quality bio-oils [7–9].

As a natural complex aromatic polymer, lignin comprises three phenylpropane units (*p*-hydroxyphenyl, guaiacyl and syringol units) which are linked by various chemical bonds [10–13]. The arylglycerol-β-aryl ether (β—O—4) is the most prominent substructure type in lignin, and significantly influences the chemical structure and physical properties of lignin [14,15].

Studies of the pyrolysis behavior of lignin have been reported over the decades. Amen-Chen et al. [16] reviewed previous experimental investigations and suggested that the lignin pyrolysis process was mainly initiated by radical reactions. Kawamoto et al. [17–19] used a custom-built pyrolysis reactor to investigate the effects of different bond types and substituents on the thermal degradation behaviors of lignin model compounds, and found that both had important effects on the cleavage and reactivity of chemical linkages. In experimental studies, the formation pathways of pyrolytic products have mainly been inferred by analysis of the product distribution. However, this method is difficult to apply for the in-depth prediction of the possible intermediates and formation pathways of major products. Density functional theory seems to be a suitable complementary approach to solve this problem. Beste et al. [20,21] calculated the bond dissociation enthalpies of phenethyl phenyl ether (PPE) with different substituents. Huang et al. [22] investigated the pyrolysis mechanism of a β—O—4 type lignin dimer model compound (1-phenyl-2-phenoxy-1,3-propanediol). However, limited studies are available on the pyrolysis mechanism of lignin model compounds by combining experimental studies with theoretical methods.

* Corresponding author. Fax: +86 27 87545526.
** Corresponding author. Fax: +86 10 61772032x801.
E-mail addresses: jashao@hust.edu.cn (J. Shao), qianglu@mail.ustc.edu.cn (Q. Lu).

http://dx.doi.org/10.1016/j.jaap.2015.07.009
0165-2370/

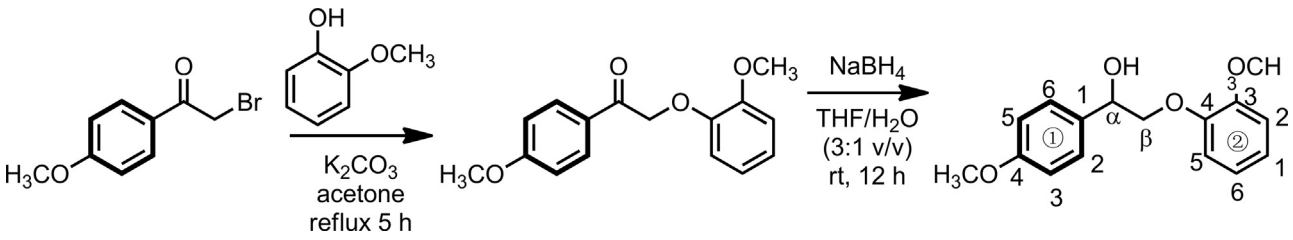

Fig. 1. Synthesis of the β—O—4 type lignin model dimer.

The objective of this research is to analyze and reveal the pyrolysis behavior and mechanism of a β—O—4 type model compound, 1-(4-methoxyphenyl)-2-(2-methoxyphenoxy) ethanol. Analytical Py-GC/MS experiments were conducted to explore the thermal degradation characteristics and product distributions. Meanwhile, DFT (M06-2X) calculations provided a theoretical support for the formation mechanisms of pyrolytic products. Finally, a comprehensive comparison of the experimental and computational results was performed to determine the pyrolysis mechanism of the β—O—4 dimer.

2. Materials and experimental methods

2.1. Lignin dimer preparation

The β—O—4 type lignin dimer compound (1-(4-methoxyphenyl)-2-(2-methoxyphenoxy) ethanol) was synthesized by the chemistry department of Peking University. The specific synthesis reactions are shown in Fig. 1, and the details can be found elsewhere [23].

2.2. Experimental methods

Analytical Py-GC/MS experiments were conducted using a pyrolyzer (CDS5200HP, CDS Analytical, Inc.) connected to a gas chromatograph/mass spectrometer (GC/MS, PerkinElmer Clarus560S). The target pyrolysis temperatures were set at 300 °C, 500 °C, or 800 °C for 20 s under helium gas (99.999%, 1 mL/min) with a heating rate of 20 °C/ms. The temperatures of the injector and transfer line were maintained at 300 °C. The pyrolytic products were separated and on-line analyzed by the GC/MS equipped with an Elite-35MS capillary column (30 m × 0.25 mm i.d., 0.25 μm film thickness). The split ratio was 80:1. The GC oven temperature was initially set at 40 °C for 2 min, and then increased to 280 °C at 15 °C/min, where it was kept for another 2 min. Mass spectrometer was operated in EI mode at 70 eV. The pyrolytic products were identified through the Wiley/NIST 2008 Registry of Mass Spectral Data. For each pyrolysis temperature, the experiments were conducted at least three times to confirm the reproducibility of the pyrolytic product distribution.

3. Computational details

All calculations were carried out using the Gaussian 09 software package [24]. To conserve computational resources, the time-consuming rigid energy scans were conducted using the B3LYP method at the 6-31+G(d) level, for the process of comparing the electron energies of model compounds with distinct spatial structures. Then, all the reactants, intermediates (IMs), transition states (TSs), and products were optimized with the precise M06-2X method at the 6-311++G(d, p) level. Furthermore, the reactants, IMs, and products were evaluated by frequency analysis at the same level to ensure their stabilities without imaginary frequencies, and the TSs were similarly evaluated to ensure unique imaginary frequencies. The thermodynamic parameters of the various species were obtained by frequency analysis under the standard condition, i.e., 298.15 K and 1 atm. The intrinsic reaction path (IRC) calculation was adopted to validate the TSs. The M06-2X method at the 6-311++G(d, p) level has been widely used for the mechanism study of lignin pyrolysis process, and its accuracy has also been previously demonstrated [20,25,26].

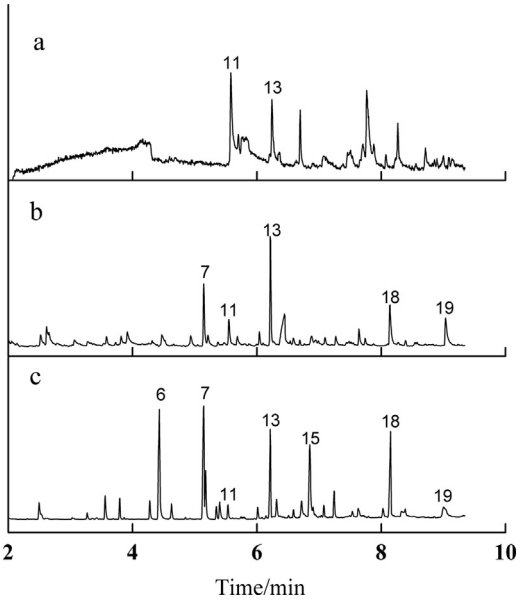

Fig. 2. The total ion chromatograms from fast pyrolysis of the lignin dimer at different temperatures: (a) 300 °C, (b) 500 °C, and (c) 800 °C.

4. Results and discussion

4.1. Py-GC/MS analysis

Fig. 2 shows the typical ion chromatograms from fast pyrolysis of the lignin dimer under three different temperatures. The relative contents of the pyrolytic products are calculated and given in Table 1. As shown in Table 1, the species of pyrolytic products are small at 300 °C, chiefly guaiacol and 4-methoxystyrene. When the pyrolysis temperature raise to 500 °C, four new products can be found in the chromatogram, i.e. 2-hydroxybenzaldehyde, 4-methoxybenzaldehyde, 4-methoxyacetophenone and 4-hydroxyacetophenone. Whereas at 800 °C, a complex product distribution is obtained, mainly consisting of various monocyclic aromatics and phenolics.

4.2. DFT calculations

4.2.1. Structure identification of the lignin dimer

The lignin dimer can adopt diverse spatial arrangements via rotations about its covalent bonds. Therefore, it is essential to deter-

Table 1
Pyrolytic product distribution at different temperatures (peak area %).

No	Residence time	Molecule	Molecular weight	Formula	300 °C	500 °C	800 °C
1	2.49	Toluene	92	c_7h_8			2.96
2	3.27	Ethylbenzene	106	c_8h_{10}			0.67
3	3.56	Styrene	104	c_8h_8			2.58
4	3.79	Anisole	108	c_7h_8o			2.03
5	4.27	Benzaldehyde	106	c_7h_6o			1.84
6	4.43	Phenol	94	c_6h_6o			16.04
7	5.15	2-Hydroxybenzaldehyde	122	$c_7h_6o_2$		18.06	14.40
8	5.18	2-Hydroxytoluene	108	c_7h_8o			4.82
9	5.35	Acetophenone	120	c_8h_8o			1.32
10	5.4	3-Methylphenol	108	c_7h_8o			2.00
11	5.54	Guaiacol	124	$c_7h_8o_2$	48.07	8.14	1.58
12	6.01	2-Ethylphenol	122	$c_8h_{10}o$			1.35
13	6.22	4-Methoxystyrene	134	$c_9h_{10}o$	25.63	28.02	9.33
14	6.32	4-Ethylphenol	122	$c_8h_{10}o$			2.39
15	6.85	4-Vinylphenol	120	c_8h_8o			11.40
16	7.08	2-Methoxybenzaldehyde	136	$c_8h_8o_2$			1.20
17	7.24	4-Methoxybenzaldehyde	136	$c_8h_8o_2$		3.64	2.96
18	8.15	4-Methoxyacetophenone	150	$c_9h_{10}o_2$		17.56	10.75
19	9.01	4–Hydroxyacetophenone	136	$c_8h_8o_2$		14.08	4.29
20		Unknown			26.30	10.50	6.10

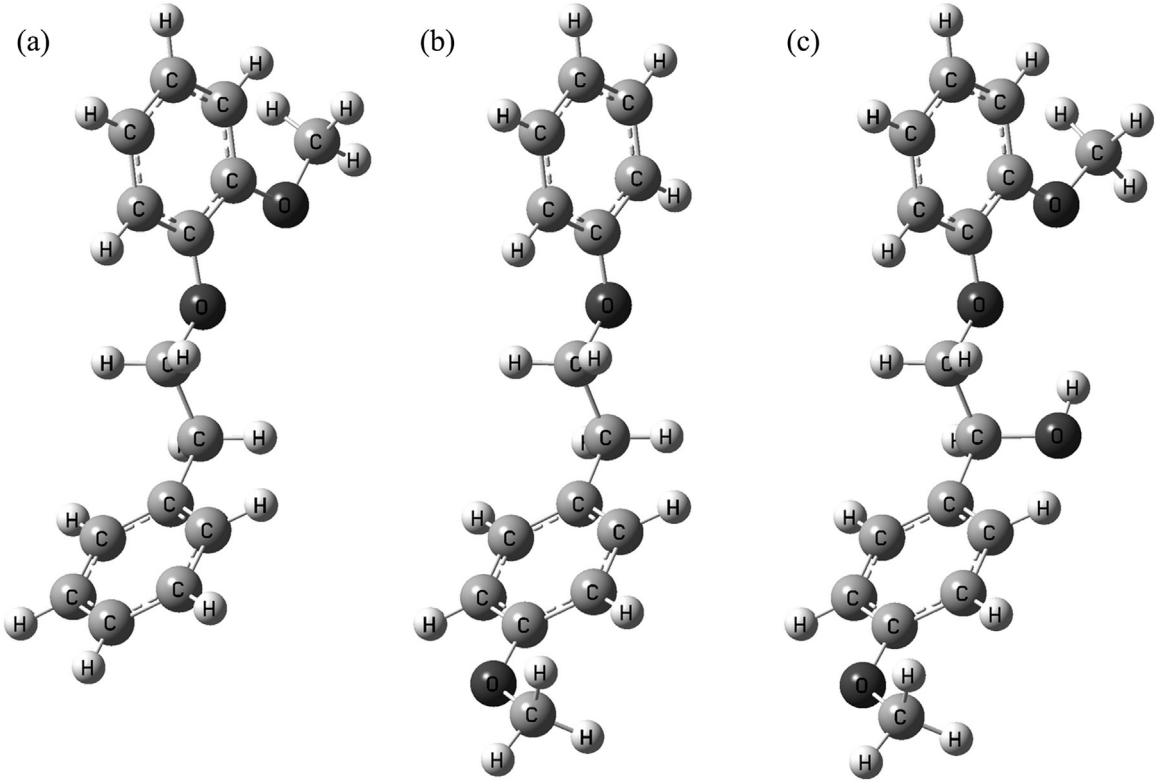

Fig. 3. Spatial structures of the lignin model compounds.

mine the lowest energy spatial arrangement. According to Beste et al. [20,27], for a PPE in which a methoxyl substituent is ortho to the site of the ether bond, the most stable structure adopts an orthogonal arrangement of the planes of the two benzene rings, with the methoxyl group located on the side of the protruding oxygen atom in the β—O—4 ether linkage, as shown in Fig. 3(a). In the case of a PPE where the methoxyl group is located para to Cα, the C atom of the methoxyl group lies in the plane of benzene ring (Fig. 3(b)). Based on the above results, we propose the structure of the lignin dimer as shown in Fig. 3(c).

To verify the correctness of the selected geometry of the lignin dimer, the energy scan process was carried out as follows. The dihedral angles of the D (Cβ—O—$C_{4'}$—$C_{2'}$), D (Cα—Cβ—O—$C_{4'}$), D (C_1—Cα—Cβ—O), and D (C_2—C_1—Cα—Cβ) were scanned by the rigid energy scanning method with a 60° step length. Based on the reference structure displayed in Fig. 3(c), the electronic energies as a function of the four dihedral angles are plotted in Fig. 4. The structure shown in Fig. 3(c) clearly has the lowest energy in the potential energy surface.

4.2.2. *Preliminary pyrolysis mechanism of the lignin dimer*

At present, the mechanism for the preliminary lignin pyrolysis is still in dispute. Beste et al. [20] suggested that the preliminary pyrolysis process mainly involved the homolysis of the Cβ—O and Cα—Cβ bonds. Kawamoto et al. [28] experimentally confirmed that other reactions could also take place during the pyrolysis of typical

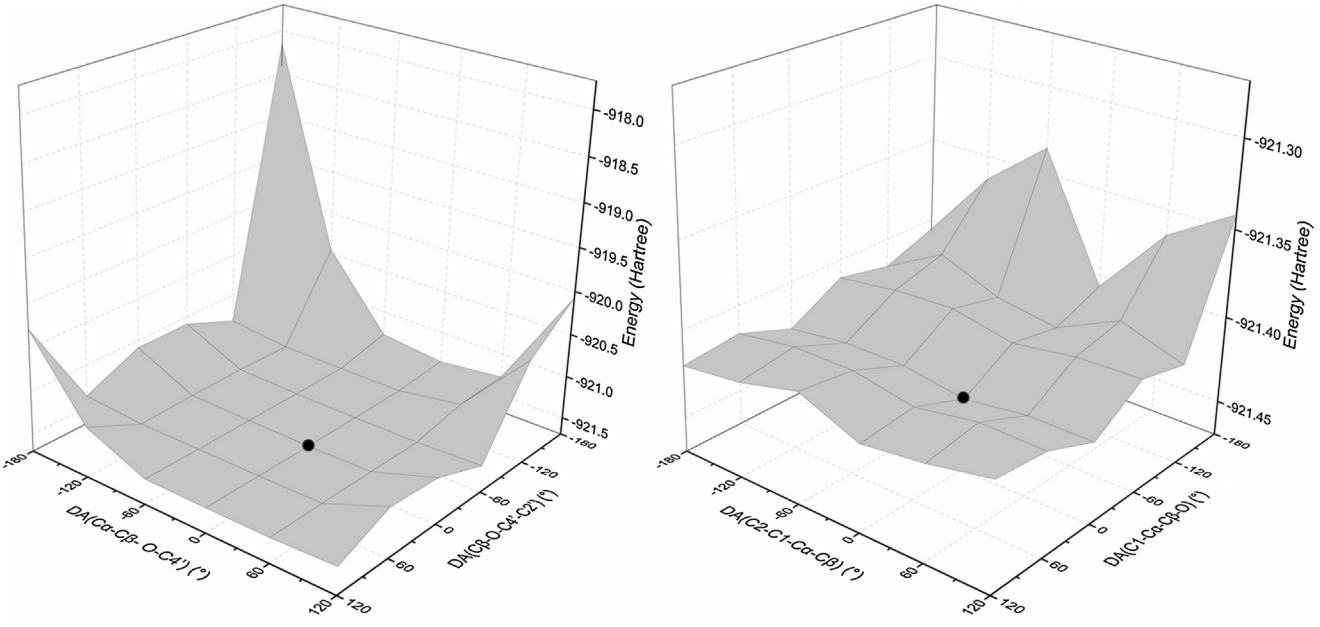

Fig. 4. The potential energy surfaces of the lignin dimer.

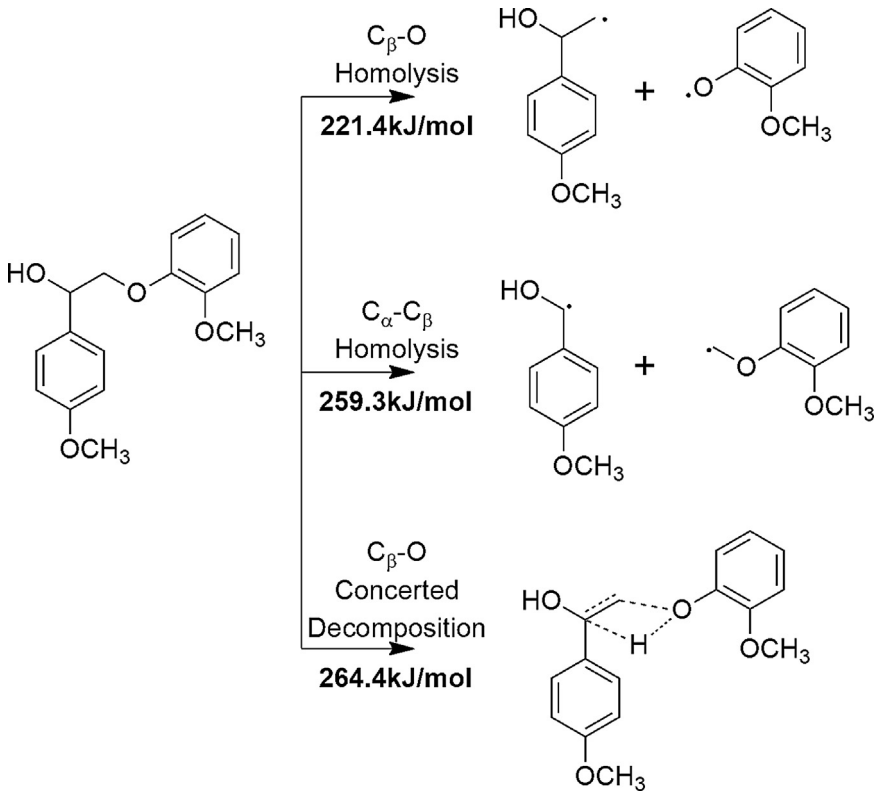

Fig. 5. Preliminary pyrolysis mechanisms of lignin dimer.

lignin model compounds. Another point considered by Korobkov et al. [29] and Amen-Chen et al. [16] was that the concerted decomposition of Cβ—O bond mainly occurred in the low-temperature process. With the increasing of the pyrolysis temperature, the proportion of the homolytic reactions increased. Therefore, in order to determine the preliminary pyrolysis mechanism of this lignin dimer, we calculated the bond dissociation energies for the Cβ—O and Cα—Cβ homolysis and energy barrier for the concerted decomposition of Cβ—O, as shown in Fig. 5. It is seen that the bond dissociation energy of Cβ—O is relatively low (221.4 kJ/mol), lower than the Cα–Cβ bond dissociation energy (259.3 kJ/mol) and the Cβ—O concerted decomposition energy barrier (264.4 kJ/mol).

4.2.3. Pyrolytic pathways based on Cβ—O homolysis

During the Cβ—O homolytic process, the Cβ—O bond is broken and the free radicals IM **a** and IM **b** are generated (Fig. 6). The subsequent reactions are illustrated in Figs. 6 and 7, respectively.

Fig. 6 shows four reaction pathways subsequent to the formation of IM **a**. In the pathway a-1, an H radical in IM **a** transfers from the Cα to the Cβ position, to generate the IM **a-1-i1**. Then, the hydroxyl radical is dehydrogenated to form **a-1-i2** (4-methoxyacetophenone), and the overall energy barrier for this reaction path is 359.9 kJ/mol. In path a-2, IM **a** undergoes a hydrogenation reaction to form IM **a-2-i1**. After overcoming the TS **a-2-ts1** with a low energy barrier, IM **a-2-i1** is dehydrated by the loss of the Cα-hydroxyl and Cβ-hydrogen radicals to produce **a-2-i2** (4-methoxystyrene). IM **a-2-i2** can undergo demethylation and subsequent hydrogenation to form **a-2-i4** (4-vinylphenol). The overall energy barrier for path a-2 is 274.9 kJ/mol. It is to note that free hydrogen radicals required for the above hydrogenation reactions can be generated during the pyrolysis process, from the dehydrogenation reaction pathways (e.g. path a-1, path b-2) as well as the coking and polyaromatic hydrocarbons formation process [30]. In path a-3, 4-methoxystyrene (**a-3-i1** or **a-2-i2**) can also be generated from IM **a** directly through dehydroxylation, but the overall energy barrier for this process is relatively high (295.9 kJ/mol), hence it is not the optimal pathway for the formation of 4-methoxystyrene. In path a-4, the C_1—Cα bond in the intermediate is broken, producing the **a-4-i1** and **a-4-i2** (vinyl alcohol); then, the **a-4-i1** can undergo a hydrogenation reaction to form **a-4-i3** (anisole). The overall energy barrier for path a-4 is 316.6 kJ/mol. According to the assessment of the overall energy barriers of different reaction pathways, the formations of intermediates **a-2-i2** (4-methoxystyrene) and **a-2-i4** (4-vinylphenol) are the most favorable due to their low energy barriers, wherein **a-2-i2** is easier to obtain because of the fewer steps along the reaction path a-2.

As shown in Fig. 7, the reactions following the generation of IM **b** occur with four major pathways. In path b-1, IM **b** undergoes hydrogenation to generate **b-1-i1** (guaiacol). Liu et al. [31] thought that the guaiacol should be the main source of phenol. Attacked by a free H radical, the guaiacol will overcome the TS **b-1-ts1** to generate IM **b-1-i2** which will undergo demethoxylation to generate phenol (**b-1-i3**). Path b-1 has a relatively low overall energy barrier of 221.4 kJ/mol. In path b-2, an H radical in the methoxyl group of the guaiacol (**b-1-i1**) is removed, generating IM **b-2-i1**. Then, IM **b-2-i1** will overcome TS **b-2-ts2**, during which process the positions of the C atom and the O atom in the methoxyl group are exchanged, generating IM **b-2-i2**. Finally, the product **b-2-i3** (2-hydroxybenzaldehyde) will be generated by the loss of one H radical. The overall energy barrier for path b-2 is 444.1 kJ/mol. In path b-3, IM **b-2-i1** can also be produced from IM **b** by overcoming TS **b-2-ts1**, during which an H radical in the methoxyl group transfers and participates in the formation of the phenolic hydroxyl group in intermediate **b-2-i1**. Then IM **b-2-i1** undergoes the same subsequent reactions as path b-2 to form **b-2-i3** (2-hydroxybenzaldehyde), and the overall energy barrier in this pathway is 351.6 kJ/mol, lower than that in the pathway b-2 (444.1 kJ/mol). In addition, we also investigated a pathway similar to the one proposed by Liu et al. [31] for producing the phenol, i.e., path b-4. In path b-4, IM **b** interacts with a free H radical to form **b-3-i1** by overcoming the TS **b-3-ts1**. Then, **b-3-i1** will successively lose the methoxyl group and undergo a hydrogenation reaction to form phenol with an overall energy barrier of 221.4 kJ/mol. The overall energy barrier of path b-4 is the same as that of path b-1, while the energy barrier of **b-1-i1**→**b-1-ts1** is lower than that of **b-3-i1**→**b-3-i2**. Therefore, path b-1 should be more favorable than path b-4. In sum, the most possible pathway from IM **b** is the path b-1, forming the product of **b-1-i1** (guaiacol) which can further decompose to form **b-2-i3** (2-hydroxybenzaldehyde) and **b-1-i3** (phenol).

4.2.4. Pyrolytic pathways based on Cα—Cβ homolysis

As shown in Fig. 8, during the Cα—Cβ homolytic process, the Cα—Cβ bond is broken, forming IM **c** and IM **d**. IM **c** can decompose along two main reaction pathways. In path c-1, an H radical is removed from IM **c** to form **c-1-i1** (4-methoxybenzaldehyde) with an overall energy barrier of 367.8 kJ/mol. In path c-2, IM **c** undergoes a hydrogenation reaction to form **c-2-i1** (4-methoxybenzenemethanol), with an overall energy barrier of 259.3 kJ/mol. After the formation of IM **d**, there may be three main subsequent reaction pathways. In path d-1, IM **d** will overcome TS **d-1-ts1** to form IM **d-1-i1**. Then, **d-1-i1** will undergo dehydrogenation to form **d-1-i2** (2-methoxybenzaldehyde) with an overall energy barrier of 333.7 kJ/mol. In path d-2, IM **d** undergoes a hydrogenation reaction, forming **d-2-i1** (1,2-dimethoxybenzene) with an overall energy barrier of 259.3 kJ/mol. In path d-3, the possibility of the dissociation of IM **d** is considered, but the overall energy barrier for loss of methylene from the IM **d** is 577.3 kJ/mol, which far exceeds those of the former two pathways, and thus, will not be further considered. In conclusion, the products most likely to be generated based on the Cα—Cβ homolysis are **d-2-i1** (1,2-dimethoxybenzene) and **c-2-i1** (4-methoxybenzenemethanol), both with the overall energy barriers of 259.3 kJ/mol.

4.2.5. Pyrolytic pathways based on Cβ—O concerted decomposition

During the Cβ—O concerted decomposition process, the lignin dimer directly generates intermediates **CR-i1** and **CR-i2** (guaiacol) via the four-membered ring TS **CR-ts1**, as shown in Fig. 9. The two intermediates can undergo further reactions. IM **CR-i1** is converted to IM **CR-i3** (4-methoxyacetophenone) via TS **CR-ts2** by the isomerization of the side chain enol to the ketone. Demethylation occurs accompanied by the formation of **CR-1-i2** (4-methoxybenzaldehyde) and **CR-2-i2** (4-hydroxyacetophenone) from IM **CR-i3**. **CR-1-i2** is equivalent to **c-1-i1** in Fig. 8. However, the overall energy barrier required for the production of **CR-1-i2** along this path is lower, and thus, the formation of **CR-1-i2** through the Cβ—O concerted decomposition is the optimal path. In addition, IM **CR-i2** can go on to produce **b-1-i3** (phenol) according to the mechanism shown in Fig. 9. Among all of the above products, IM **CR-i1** has an unstable enol structure which is prone to undergo isomerization to produce IM **CR-i3** (4-methoxyacetophenone). Therefore, **CR-i3** (4-methoxyacetophenone) and **CR-i2** (guaiacol) should be the major products from the Cβ—O concerted decomposition. Other products can be generated by subsequent thermal decomposition reactions.

4.2.6. Summary of pyrolysis mechanism and products of the lignin dimer

According to the above discussions, a summary of the pyrolysis mechanisms and pathways of the lignin dimer can be drawn, as shown in Fig. 10. Based on the optimal reaction pathways and formation sequences for each product, the pyrolytic products can be classified into two types: 1. principal products which are generated from the preliminary pyrolysis process and have low reaction energy barriers; and 2. minor products which are produced in the late stages and have high energy barriers.

As shown in Fig. 10, the pyrolytic products based on the three preliminary pyrolysis mechanisms are substantially different. The principal products from the Cβ–O homolysis are guaiacol (**b-1-i1**) and 4-methoxystyrene (**a-2-i2**). Those from the Cα—Cβ homolysis are 1,2-dimethoxybenzene (**d-2-i1**) and 4-

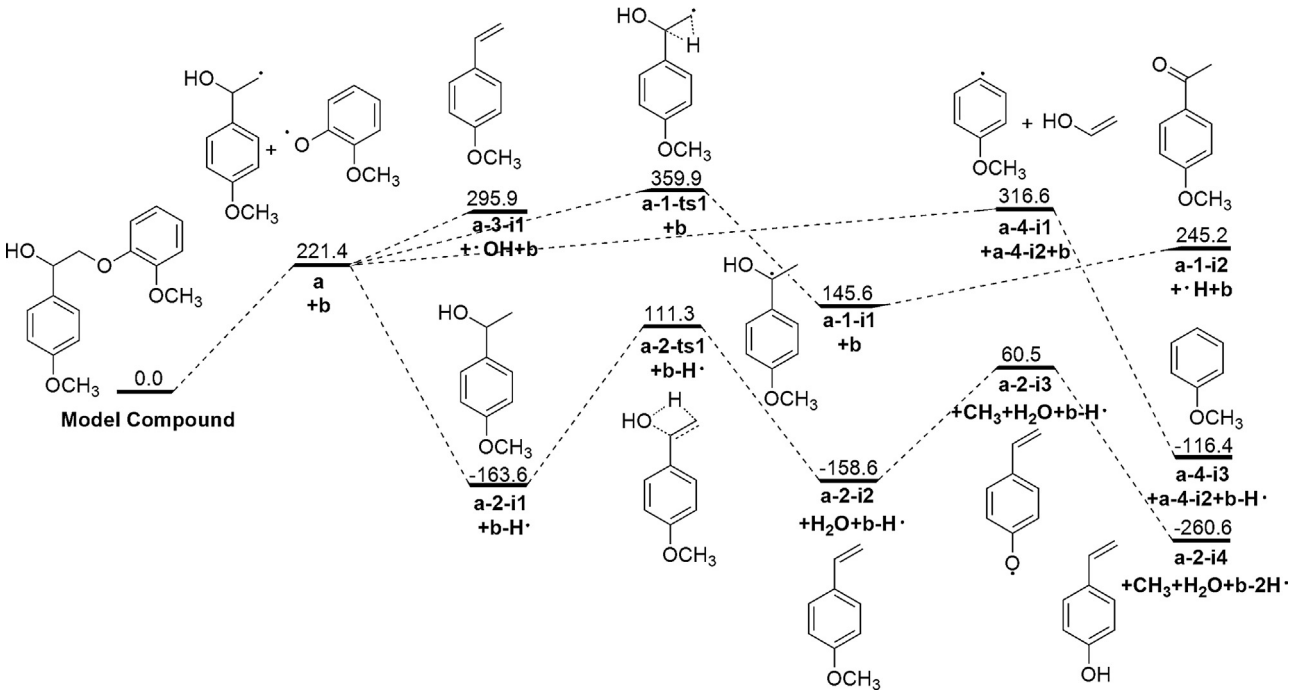

Fig. 6. The possible subsequent reaction pathways following the radical **a** from the Cβ—O homolysis.

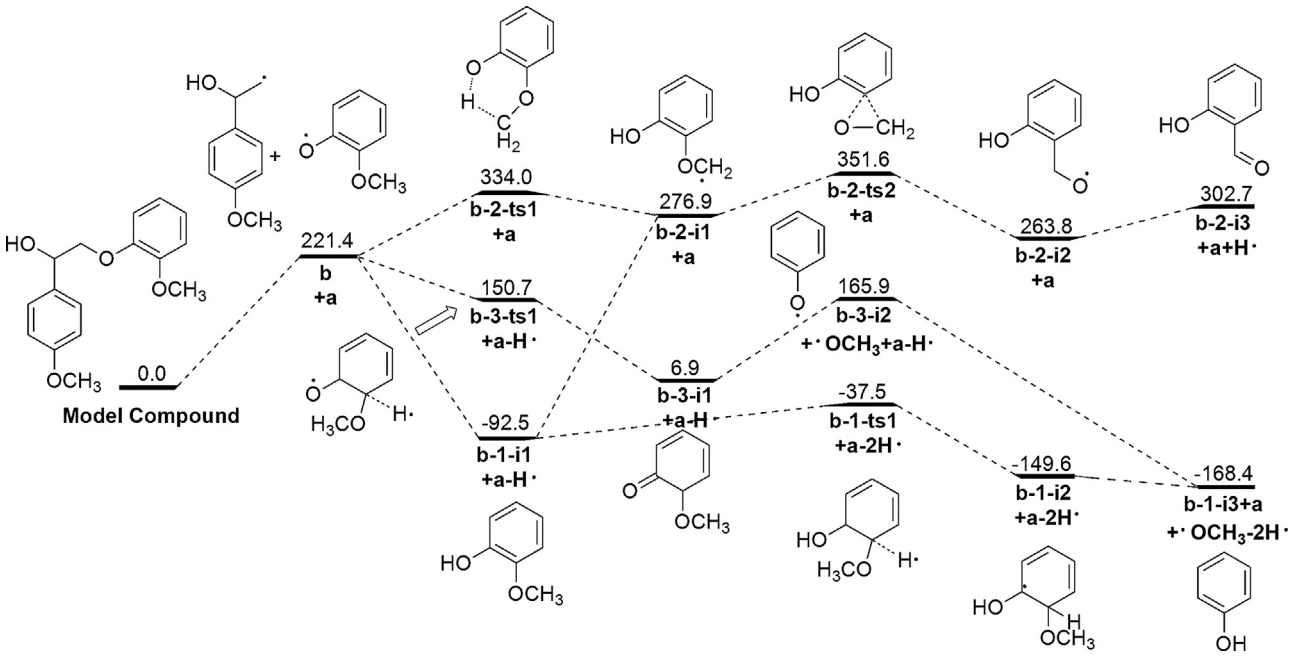

Fig. 7. The possible subsequent reaction pathways following the radical **b** from the Cβ—O hemolysis.

methoxybenzenemethanol (**c-2-i1**). The principal products from the Cβ—O concerted decomposition are guaiacol (**CR-i2**) and 4-methoxyacetophenone (**CR-i3**). In terms of energy barriers, the Cβ—O homolytic reaction requires the lowest energy compared to the Cα—Cβ homolytic and Cβ—O concerted decomposition reactions. From this standpoint, the Cβ—O homolytic mechanism is the most favorable. However, the difference of the energy barriers between the Cα—Cβ homolysis and the Cβ—O concerted decomposition is quite small. Hence, it is difficult to directly determine which mechanism is more preferable without experimental data. In addition, it is worth noting that the above-illustrated pyrolytic mechanisms and products are based on the preliminary pyrolysis of the lignin dimer. During the real pyrolysis process, the lignin dimer, intermediate radicals and primary products will proceed via different reactions, such as bimolecular hydrogen abstraction [21], oxygen–carbon phenyl migration [32], carbon–carbon phenyl migration [33] and secondary cracking reactions, which will affect the final pyrolytic product distribution. These processes are not taken into account in this paper, and will be investigated in the future.

4.2.7. Comparison of experimental and theoretical results

As demonstrated in Table 1, the major pyrolytic products produced at the low temperature (300 °C) are guaiacol (**b-1-i1**) and

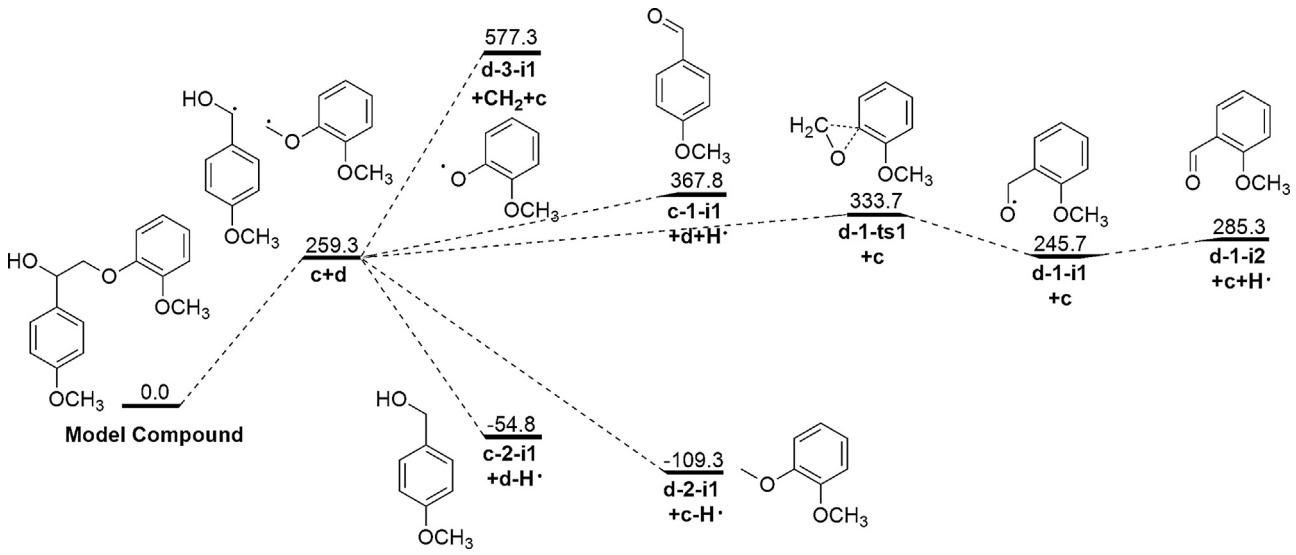

Fig. 8. The possible reaction pathways from the Cα—Cβ homolysis.

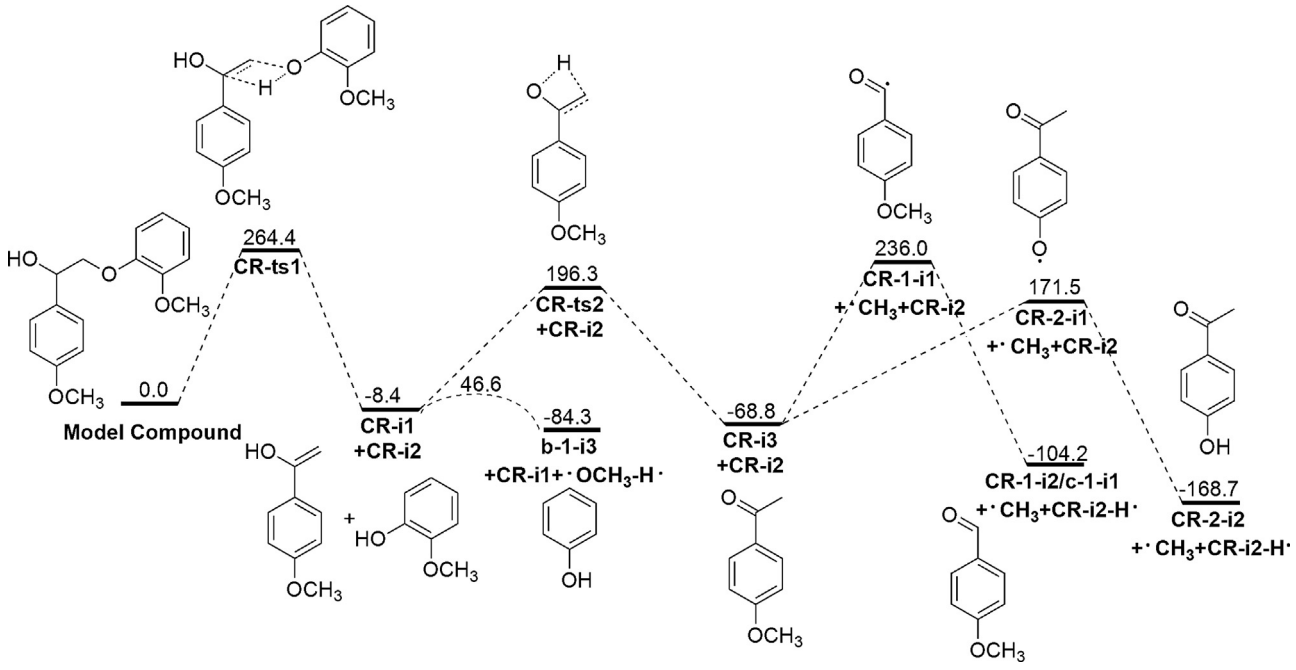

Fig. 9. The possible reaction pathways from Cβ—O concerted decomposition.

4-methoxystyrene (**a-2-i2**). From the DFT calculations, the two substances are the dominant end products of the Cβ—O homolytic reaction with the lowest energy barriers. Therefore, we can determine that the main reaction mechanism for the low-temperature pyrolysis of the lignin dimer is the Cβ—O homolytic reaction. The results agree well with the findings by Britt et al. [34] who confirmed that Cβ—O homolytic reaction was more favorable than Cβ–O concerted decomposition reaction in the pyrolysis of *o*-CH_3O-PPE. However, Huang et al. [22] obtained the opposite results when investigating the temperature effect on pyrolysis of β—O—4 type lignin dimer model compound. They found that the concerted decomposition reactions would dominate over free-radical homolytic reactions at low temperatures, while at high temperatures the free-radical reactions (C–O homolysis) would dominate over the concerted decomposition reactions. The different results in these studies might be attributed to the different model compound structures. The lignin model compound selected by Huang et al. [22] has no methoxyl group on the phenyl ring adjacent to the ether oxygen, and it has been confirmed that the presence of the methoxyl group can enhance the Cβ—O homolysis while have little effect on Cβ—O concerted decomposition [34].

At medium temperature (500 °C), the number of pyrolytic products increases. Compared with the product distribution from 300 °C, the relative content of guaiacol (**b-1-i1**) decreases, while the amount of 2-hydroxybenzaldehyde (**b-2-i3**) increases, an indication of the further decomposition of the guaiacol. Meanwhile, a great number of carbonyl-containing compounds, such as 4-methoxyacetophenone (**CR-i3**), 4-methoxybenzaldehyde (**CR-1-i2**), and 4-hydroxyacetophenone (**CR-2-i2**), are found. Coupled with the theoretical analysis, these substances are mainly generated through the Cβ—O concerted decomposition reaction. Since the energy barrier of the Cβ—O concerted decomposition reaction

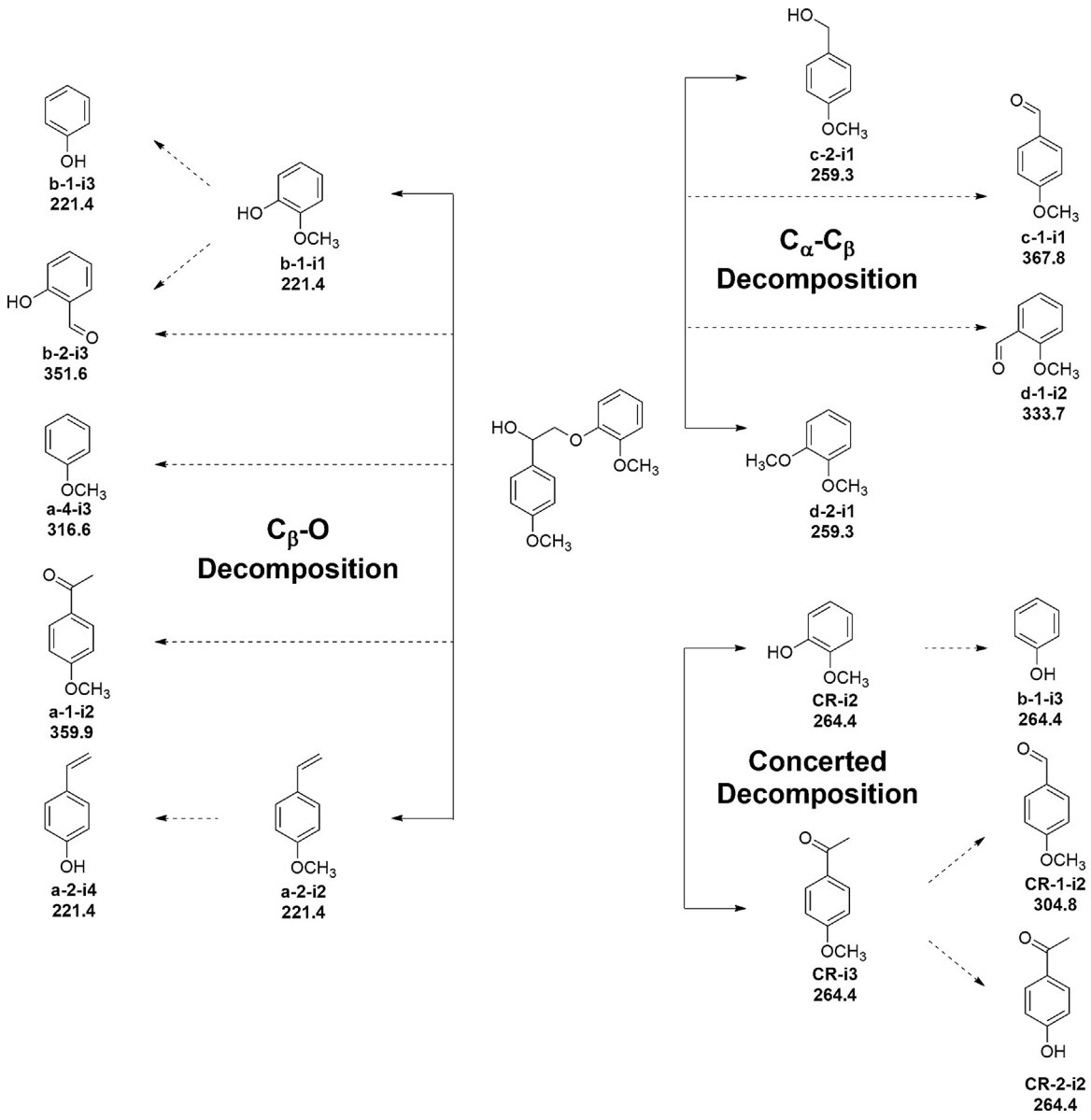

Fig. 10. Summary of pyrolytic pathways of the lignin dimer.

is higher than that of the Cβ–O homolytic reaction, it implies that the Cβ—O concerted decomposition reaction is prominent in the thermal degradation of the lignin dimer under medium pyrolysis temperatures.

At high temperature (800 °C), various small molecular substances will be formed. According to the theoretical analysis, the products formed from Cβ—O homolysis and Cβ—O concerted decomposition undergo dissociation reactions, producing these minor products.

As the theoretical analysis shows, the energy barrier of the Cα—Cβ homolytic reaction is slightly lower than that of the Cβ—O concerted decomposition. However, Cα—Cβ homolytic products such as 1,2-dimethoxybenzene (**d-2-i1**) and 4-methoxybenzenemethanol (**c-2-i1**), were not detected experimentally. Therefore, it is able to infer that the Cα—Cβ homolytic mechanism is not applicable in the actual pyrolysis process.

5. Conclusions

In this research, the pyrolysis mechanism and product distribution of a β—O—4 type lignin dimer (1-(4-methoxyphenyl)-2-(2-methoxyphenoxy) ethanol) was investigated by analytical Py-GC/MS experiments and DFT calculations. The results show that 4-methoxystyrene and guaiacol are the major products through Cβ-O homolytic mechanism at low temperatures. Cβ-O homolysis and Cβ—O concerted decomposition mechanisms co-dominate the reactions at moderate temperatures, producing 4-methoxystyrene, carbonyl-containing substances and guaiacol. At high temperatures, the products obtained from Cβ—O homolysis and Cβ—O concerted decomposition undergo secondary thermal cracking, generating a large number of small molecule products which result in the complexity of the pyrolytic products.

Acknowledgements

The authors greatly appreciate financial support from the National Basic Research Program of China (2013CB228102), the National Natural Science Foundation of China (51376075), the Special Fund for Agro-scientific Research in the Public Interest (201303095), the Foundation of State Key Laboratory of Coal Combustion (FSKLCC1413A), the Independent Innovation Foundation of Huazhong University of Science and Technology (2014TS118) and the experiment was also assisted by the Analytical and Testing Center at Huazhong University of Science & Technology (http://atc.hust.edu.cn). Mr. Yangyang Wu helped improve the linguistic presentation of the manuscript.

References

[1] D.R. Dodds, R.A. Gross, Chemicals from biomass, Science 318 (2007) 1250.
[2] A.V. Bridgwater, Review of fast pyrolysis of biomass and product upgrading, Biomass Bioenergy 38 (2012) 68.
[3] Z. Tang, Q. Lu, Y. Zhang, X. Zhu, Q. Guo, One step bio-oil upgrading through hydrotreatment, esterification, and cracking, Ind. Eng. Chem. Res. 48 (2009) 6923.
[4] Z. Wang, Q. Lu, X.F. Zhu, Y. Zhang, Catalytic fast pyrolysis of cellulose to prepare levoglucosenone using sulfated zirconia, ChemSusChem 4 (2011) 79.
[5] D. Fabbri, C. Torri, I. Mancini, Pyrolysis of cellulose catalysed by nanopowder metal oxides: production and characterisation of a chiral hydroxylactone and its role as building block, Green Chem. 9 (2007) 1374.
[6] Q. Lu, W.-M. Xiong, W.-Z. Li, Q.-X. Guo, X.-F. Zhu, Catalytic pyrolysis of cellulose with sulfated metal oxides: a promising method for obtaining high yield of light furan compounds, Bioresour. Technol. 100 (2009) 4871.
[7] G. Xu, S. Huang, Y. Yang, Y. Wu, K. Zhang, C. Xu, Techno-economic analysis and optimization of the heat recovery of utility boiler flue gas, Appl. Energy 112 (2013) 907.
[8] R. Vinu, L.J. Broadbelt, A mechanistic model of fast pyrolysis of glucose-based carbohydrates to predict bio-oil composition, Energy Environ. Sci. 5 (2012) 9808.
[9] H.B. Mayes, L.J. Broadbelt, Unraveling the reactions that unravel cellulose, J. Phys. Chem. A 116 (2012) 7098.
[10] J.H. Lora, W.G. Glasser, Recent industrial applications of lignin: a sustainable alternative to nonrenewable materials, J. Polym. Environ. 10 (2002) 39.
[11] Q. Liu, S. Wang, Y. Zheng, Z. Luo, K. Cen, Mechanism study of wood lignin pyrolysis by using TG–FTIR analysis, J. Anal. Appl. Pyrolysis 82 (2008) 170.
[12] J. Hu, D. Shen, R. Xiao, S. Wu, H. Zhang, Free-radical analysis on thermochemical transformation of lignin to phenolic compounds, Energy Fuels 27 (2012) 285.
[13] T. Nakamura, H. Kawamoto, S. Saka, Pyrolysis behavior of Japanese cedar wood lignin studied with various model dimers, J. Anal. Appl. Pyrolysis 81 (2008) 173.
[14] T. Kishimoto, Y. Uraki, M. Ubukata, Easy synthesis of βO4 type lignin related polymers, Org. Biomol. Chem. 3 (2005) 1067.
[15] M. Bardet, D. Robert, K. Lundquist, S. von Unge, Distribution of erythro and threo forms of different types of βO4 structures in aspen lignin by 13C NMR using the 2D INADEQUATE experiment, Magn. Reson. Chem. 36 (1998) 597.
[16] C. Amen-Chen, H. Pakdel, C. Roy, Production of monomeric phenols by thermochemical conversion of biomass: a review, Bioresour. Technol. 79 (2001) 277.
[17] H. Kawamoto, T. Nakamura, S. Saka, Pyrolytic cleavage mechanisms of ligninether linkages: a study on *p*-substituted dimers and trimers, Holzforschung 62 (2008) 50.
[18] H. Kawamoto, S. Horigoshi, S. Saka, Pyrolysis reactions of various lignin model dimers, J. Wood Sci. 53 (2007) 168.
[19] H. Kawamoto, S. Horigoshi, S. Saka, Effects of side-chain hydroxyl groups on pyrolytic β-ether cleavage of phenolic lignin model dimer, J. Wood Sci. 53 (2007) 268.
[20] A. Beste, A. Buchanan III, Computational study of bond dissociation enthalpies for lignin model compounds. Substituent effects in phenethyl phenyl ethers, J. Org. Chem. 74 (2009) 2837.
[21] A. Beste, A. Buchanan Iii, R.J. Harrison, Computational prediction of α/β selectivities in the pyrolysis of oxygen-substituted phenethyl phenyl ethers, J. Phys. Chem. A 112 (2008) 4982.
[22] J. Huang, C. Liu, D. Wu, H. Tong, L. Ren, Density functional theory studies on pyrolysis mechanism of βO4 type lignin dimer model compound, J. Anal. Appl. Pyrolysis 109 (2014) 98.
[23] J.M. Nichols, L.M. Bishop, R.G. Bergman, J.A. Ellman, Catalytic CO bond cleavage of 2-aryloxy-1-arylethanols and its application to the depolymerization of lignin-related polymers, J. Am. Chem. Soc. 132 (2010) 12554.
[24] M.J. Frisch, H.B. Schlegel, G.E. Scuseria, M.A. Robb, J.R. Cheeseman, Gaussian, Inc, Pittsburgh, (2009).
[25] R. Parthasarathi, R.A. Romero, A. Redondo, S. Gnanakaran, Theoretical study of the remarkably diverse linkages in lignin, J. Phys. Chem. Lett. 2 (2011) 2660.
[26] S. Kim, S.C. Chmely, M.R. Nimlos, Y.J. Bomble, T.D. Foust, R.S. Paton, G.T. Beckham, Computational study of bond dissociation enthalpies for a large range of native and modified lignins, J. Phys. Chem. Lett. 2 (2011) 2846.
[27] A. Beste, A. Buchanan III, Substituent effects on the reaction rates of hydrogen abstraction in the pyrolysis of phenethyl phenyl ethers, Energy Fuels 24 (2010) 2857.
[28] H. Kawamoto, M. Ryoritani, S. Saka, Different pyrolytic cleavage mechanisms of βether bond depending on the side-chain structure of lignin dimers, J. Anal. Appl. Pyrolysis 81 (2008) 88.
[29] V.Y. Korobkov, E.N. Grigorieva, V.I. Bykov, O.V. Senko, I.V. Kalechitz, Effect of the structure of coal-related model ethers on the rate and mechanism of their thermolysis: 1. Effect of the number of methylene groups in the R (CH_2) n O (CH_2) m R structure, Fuel 67 (1988) 657.
[30] M. Asmadi, H. Kawamoto, S. Saka, The effects of combining guaiacol and syringol on their pyrolysis, Holzforschung 66 (2012) 323.
[31] C. Liu, Y. Zhang, X. Huang, Study of guaiacol pyrolysis mechanism based on density function theory, Fuel Process. Technol. 123 (2014) 159.
[32] A. Beste, A.C. Buchanan, Kinetic analysis of the phenyl-shift reaction in βO4 lignin model compounds: a computational study, J. Org. Chem. 76 (2011) 2195.
[33] A. Beste, A.C. Buchanan, Role of carbon–carbon phenyl migration in the pyrolysis mechanism of betaO4 lignin model compounds: phenethyl phenyl ether and alpha-hydroxy phenethyl phenyl ether, J. Phys. Chem. A 116 (2012) 12242.
[34] P.F. Britt, A.C. Buchanan, M.J. Cooney, D.R. Martineau, Flash vacuum pyrolysis of methoxy-substituted lignin model compounds, J. Org. Chem. 65 (2000) 1376.